"Gheorghe Asachi" Technical University of Iasi, Romania

INFLUENCE OF COAL MACERALS ON BIOMETHANE PRODUCTION

Hongyu Guo[1,2,3], Yunsong Li[1], Shanlai Chen[1], Guojun Zhao[1], Daping Xia[1,3]*

[1]*School of Energy Science and Engineering, Henan Polytechnic University, Jiaozuo 454000, China*
[2]*State Key Laboratory Cultivation Base for Gas Geology and Gas Control, Henan Polytechnic University, Jiaozuo 454000, China*
[3]*Collaborative Innovation Center of Coalbed Methane and Shale Gas for Central Plains Economic Region, Henan Province, Jiaozuo 454000, China*

Abstract

In order to investigate the influence of coal macerals on biomethane production, two types of coal samples were collected respectively from Malan mine in Gujiao and Shaqu mine in Liulin, Shanxi. The vitrinite, inertinite and liptinite were separated by the methods of hand picking and float-and-sink test. Meanwhile, biomethane production experiments using the raw coal samples, vitrinite-rich coal samples, inertinite-rich coal samples as substrates were carried out in the laboratory. Finally, the fourier transform infrared spectrometer (FTIR) was used to analyze the relationship between the macerals and biomethane production. The results show that vitrinite-rich coal samples have the largest biomethane production followed by raw coals samples and inertinite-rich coal samples. Vitrinite-rich coal samples have the highest contents of aliphatic hydrocarbon and lowest degree of aromatization, while inertinite-rich coal samples have the least contents of aliphatic hydrocarbon and highest degree of aromatization. Therefore, the contents of aliphatic hydrocarbon and aromatization degree in coal with different macerals are important indicators of influencing the biomethane production potential.

Key words: biomethane, coalbed methane, degree of aromatization, functional groups, macerals

Received: August, 2013; Revised final: July, 2014; Accepted: July, 2014; Published in final edited form: June 2018

1. Introduction

Coalbed methane (CBM) development provides access to clean energy, reduces coal mine gas disasters and cuts back on greenhouse gas (GHG) emissions. Reduction of GHG is of great importance to China's fulfillment of its promises on emission reduction for the *Paris Agreement* which went into effect November 2016. Biomass waste rich in carbohydrates, such as buffalo manure, orange peel and straw, can be used to produce biomethane based on anaerobic fermentation theory (Carotenuto et al., 2016; Calabrò et al., 2017; Fersiz et al., 2017; Vasmara and Marchetti, 2016). As an important component of coalbed methane resources, biomethane may also be generated through the anaerobic fermentation process of the indigenous bacteria with coal as the substrate. The formation of biomethane is simultaneously affected by numerous factors such as temperature, pH, coal particle size, coal rank, reservoir characteristics (e.g., pore, fracture) surfactants, external chemical solvent (e.g., acetate, carbonate, N,N-dimethylformamide), H_2/CO_2, water flow, trace elements (e.g., iron, cobalt, nickel), some intermediates (e.g. fatty acids) and microbial communities (Colosimo et al., 2016; Fallgren et al., 2013; Flores, 2014; Gilcrease and Shurr, 2007; Green et al., 2008; Guan, 1990; Guo et al., 2014; Guo et al., 2017; Moore, 2012; Papendick et al., 2011; Penner et al., 2010; Strąpoć et al., 2011; Su et al., 2011; Susilawati et al., 2013; Ulrich and Bower, 2008; Wang et al., 2015; Xia et al., 2012).

Previous research evidenced that maceral groups have different properties in physical properties (e.g., hardness, color, gloss, density) and chemical properties (e.g. element content, molecular structure, chemical functional groups and antioxidant) (Mastalerz and Bustin, 1993a; Van Krevelen, 1961). The ¹³C-NMR results ever confirmed that long chain alkyl group and short chain of -CH₂ and -CH exist in

the vitrinite group and keep a relatively higher aliphatic carbon content, whereas the inertinite group consist of more aromatic carbon (Sun et al., 2003; Xie, 2002). High-resolution transmission electron microscopy (HRTEM) study shown that with an increase in coal rank, the average length of the basic structural unit (BSU) and the average number of condensed aromatic rings of vitrinite would increase (Zhao et al., 1995). Infrared spectroscopy is often used to characterize the chemical structure of the macerals in coal (Brenner, 1984; Guo et al., 1996; Ibarra et al., 1994, 1996; Kister et al., 1990; Lin and Ritz, 1993a, b; Mastalerz and Bustin, 1993a, 1993b, 1996; Mazzeo and Joseph, 2007; Millais and Murchison, 1969; Morga, 2010; Rochdi and Landais, 1991; Sun, 2005; Tschamiler and Ruiter, 1966; Walker and Mastalerz, 2004). Within the three maceral groups, liptinite generally exhibits the lowest aromaticity, the longest aliphatic chains having the least amount of branching. In contrast, inertinite shows the highest aromaticity and degree of condensation of aromatic domains. Vitrinite generally exhibits intermediate characteristics between liptinite and inertinite (Chen and Zhang, 2012; Duan et al., 2004; Guo and Bustin, 1998; Shu et al., 1996). Wang et al. (1992) combines FTIR and electron paramagnanetic resonance(EPR) to find that the aliphatic substituent group and chelate quinone group contents in the vitrinite are higher that of semivitrinite and inertinite, the free radical concentration of vitrinite, semivitrinite and inertinite is 3.87×10^{18} spins/g, 18.98×10^{18} spins/g, and 40.10×10^{18} spins/g respectively, free radicals in vitrinite belong to small oxygen-bearing aromatic π

types, and those in inertinite are large armotic π ones.

In this paper, two types of coal samples were collected respectively from Malan mine in Gujiao and Shaqumine in Liulin, Shanxi and the relationship between the functional groups in the macerals and biomethane production were test in the laboratory. The research results provide theoretical support for the optimization of field test area.

2. Materials and methods

2.1. Coal samples

Fresh chunk coal samples were collected from Malan mine in Gujiao, and Shaqu mine in Liulin, Shanxi follow the (Fig. 1). When the coal sample was grasped, it was quickly sealed in a glass pot with prepared reducing agent and desiccant. Table 1 shows the sample information and proximate analysis results.

2.2. Methanogenic bacteria

The indigenous bacteria were cultured from fresh mine water. The water was collected with sterilized plastic drum in the underground and then quickly sealed and transported to the lab, and stored in the refrigerator at 4 °C. The following culture medium was used for bacterial enrichment.

(a) Tace element solution, triglycolamic acid 1.5 g, $MnSO_4 \cdot 2H_2O$ 0.5 g, $MgSO_4 \cdot 7H_2O$ 3.0 g, $FeSO_4 \cdot 7H_2O$ 0.1 g, NaCl 1.0 g, $CoCl_2 \cdot 6H_2O$ 0.1 g, $CaCl_2 \cdot 2H_2O$ 0.1 g, $CuSO_4 \cdot 5H_2O$ 0.01 g, $ZnSO_4 \cdot 7H_2O$ 0.1 g, H_3BO_3 0.01 g, $AlK(SO_4)_2$ 0.01 g, $NiCl_2 \cdot 6H_2O$ 0.02 g, Na_2MoO_4 0.01 g per liter of distilled water.
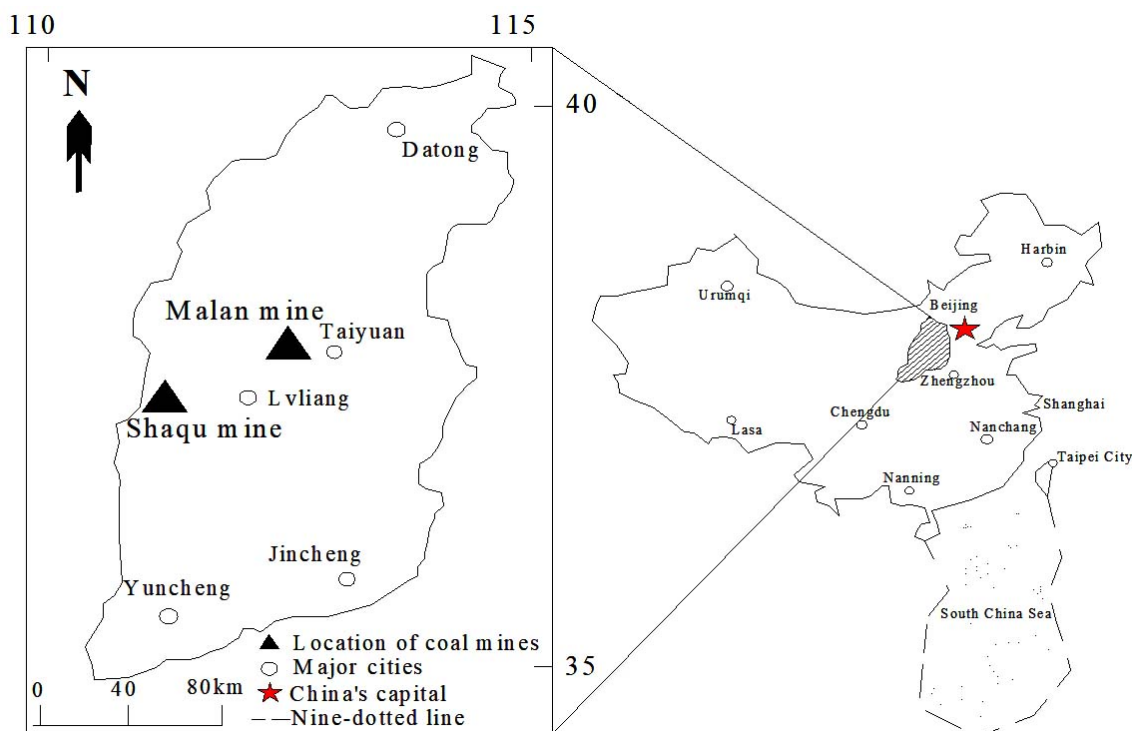

Fig. 1. Map showing location of Malan mine and Shaqu mine in Shanxi (black triangle), China's capital (red pentagon), and nearby major cities in China (white circle)

Table 1. Geological information and proximate analysis of the coal sample**s**

Sample source	Coal seam	Age	Proximate analysis			Reflectance %
			$A_{ad}\%$	$A_{ad}\%$	$A_{ad}\%$	
Malan mine in Gujiao	No.2	E. Permian-Taiyuan Formation	5.98	8.85	27.24	1.10
Shaqu mine in Liulin	No.4	E. Permian-Shanxi Formation	22.31	2.09	8.32	1.51

M, moisture; V, volatile matter; A, ash yield; ad, air dry basis; daf, dry and ash-free basis

(b) Methanogens enrichment medium

1.0 g NH_4Cl, 0.1 g $MgCl_2 \cdot 6H_2O$, 0.4 g $K_2HPO_4 \cdot 3H_2O$, 0.2 g KH_2PO_4, 0.2 g Na_2S, 2.0 g $NaHCO_3$, 0.001 g $C_{12}H_7NO_4$, 0.5 g $C_3H_7NO_2S$, 2.0 g $HCOONa$, 2.0 g CH_3COONa, 1.0 g Yeast extract, 0.1 g tryptone and 10 mL trace element solution per liter of fresh mine water.

2.3. Separation of macerals

The macerals were separated by the method of hand picking and float-and-sink test. Coal samples were sieved by a pulverizer and standard sieve to the effect that 90% of the particles are between 0.1 and 0.5mm in size and the rest are smaller than 0.1mm. Then, the maceral compositions were separated with the $ZnCl_2$ specific gravity liquid following the Chinese National Standard GB/T478 (2008) (Chen, 2012; Zhou, 2013), aiming at obtaining the vitrinite-rich and inertinite-rich coal samples.

The separated maceral compositions were repeatedly rinsed and filtered until there was no precipitation of silver chloride despite the addition of silver nitrate. After that, the samples were dried and prepared into polished powder coal following the

Chinese National Standard GB/T 16773 (2008). The maceral compositions and mineral frequencies were acquired using the Axioskop 40 Pol polarizing microscope following the Chinese National Standard GB/T 8899 (2013). The vol.% of each maceral (excluding the minerals) are shown in Table 2. The results of ultimate analysis are shown in Table 3.

2.4. Experiment setup

The methanogens was enriched and cultured according to the preparation method of culture medium. Triangular flasks with the volume of 250mL were used as the reaction bottle and the gas collector. The bottles were sealed with rubber stoppers and sealing films. The gas was collected by water displacement and the gas production was calculated by the volume of water in the collector.

The experimental device is shown in Fig. 2. Each sample (Table 2) of 20g was weighed and added with 200mL of mine water after 4d of enrichment. Two parallel experiments were conducted for each sample and the average value was taken. Meanwhile, a blank control experiment with only the culture was set.

Table 2. Quantitative statistics of macerals in coal samples (% vol.)

Sample number	Samples	Quantitative statistics		
		Vitrinite	Inertinite	Liptinite
ML-R	Raw Malan coal	78	18	4
ML-V	Vitrinite-rich Malan coal	85	12	3
ML-I	Inertinite-rich Malan coal	64	32	4
SQ-R	RawShaqu coal	74	18	8
SQ-V	Vitrinite-rich Shaqu coal	85	9	5
SQ-I	Inertinite-rich Shaqu coal	62	24	14

Table 3. The ultimate analysis of different samples

Sample number	$C_{daf}\%$	$H_{daf}\%$	$O_{daf}\%$	$N_{daf}\%$	$S_{daf}\%$
ML-R	90.39	4.69	2.82	0.48	1.63
ML-V	88.23	5.33	3.89	0.39	2.16
ML-I	89.92	4.21	4.02	0.39	1.45
SQ-R	91.20	4.51	3.30	0.46	0.53
SQ-V	87.38	5.30	6.53	0.17	0.63
SQ-I	90.35	4.22	4.36	0.49	0.58

The biomethane generation device was sealed and relocated within an incubator at 35℃ for 60 days.
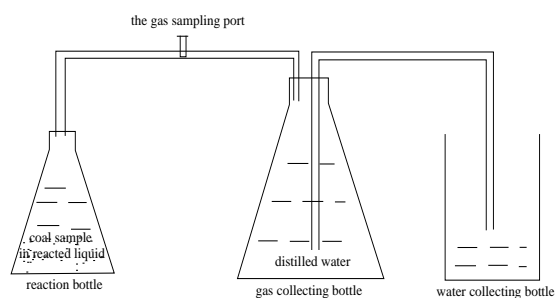

Fig. 2. Schematic diagram of biomethane generation device

2.5. Analysis method

Methane was quantified using a gas chromatograph (Agilent 7890 GC; Agilent Technologies Inc., Santa Clara, CA, USA) equipped with a Carbonplot chromatographic column (60 m × 320 μm × 1.5 μm) and a 200 °C TCD detector. The injection volume was 0.5 mL a 1-mL airtight with a 1-mL airtight syringe.

The AVATAR360 Fourier Transform Infrared Spectrometer was used to analyze the functional groups of samples (Thermo Fisher Scientific K.K., Yokohama, Japan). The instrument used a high-brightness ceramic light source, high-efficiency optical components, and a high-sensitivity DLAYGS detector. The scan range is 400 to 4000 cm^{-1}, the number of scans is 32, and the resolution is 4. Before the test, 100 mg of potassium bromide reagent and 1 mg sample was added into the agate mortar. The mixture was grinded to powder and moved into a mold, then the mold was placed on the tabletting machine with 90 kg pressure for about 5 min, and the mixture was compressed to 0.1~1 mm translucent flake for testing.

3. Results

3.1. Biomethane production

The gas compositions was measured after 60 days. Biomethane production is obtained by multiplying the total biogas production with methane concentration. The biomethane production for each sample in the Fig. 3 has been subtracted from the blank sample. Biomethane production effect of the samples from Malan mine was analyzed according to Fig. 3(a). Vitrinite-rich Malan coal sample (ML-V) has the largest CH$_4$ production of 83.89 μmol·g^{-1}. Raw Malan coal sample (ML-R) produced 50.53 μmol·g^{-1}, while the inertinite-rich Malan coal sample (ML-I) only generated 4.79μmol·g^{-1} methane. Fig. 3(b) shows the biomethane yield of the samples from Shaqu mine, obviously, vitrinite-rich Shaqu coal sample(SQ-V) has the largest CH$_4$ production of 45.75 μmol·g^{-1} compared to raw Shaqu coal sample (SQ-R) and inertinite-rich Shaqu coal sample (SQ-I). Samples separated from Malan mine and Shaqu mine shown an

interesting phenomenon that vitrinite-riched coal samples(ML-V, SQ-V) have a higher methanogenic capacity than raw coal samples(ML-R, SQ-R) and inertinite-riched coal samples(ML-I, SQ-I).
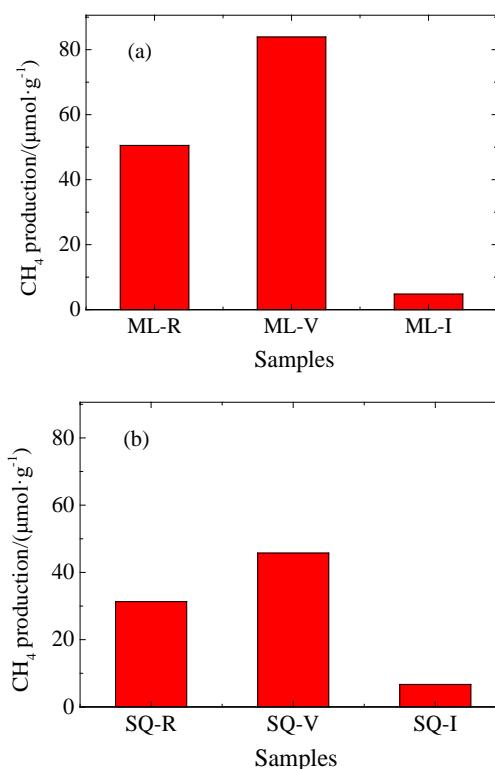

Fig. 3. CH$_4$ production of samples from Malan mine and Shaqu mine

3.2. Analysis of the chemical functional groups in the macerals

The peak area was obtained by Gaussian fitting to compare the variation characteristics of the functional groups (Fig. 4). Table 4 shows the assignment and area of the functional groups in the FTIR spectrum of samples with different proportions of macerals.

Combined with previous studies (Brown and Lander, 1960; Solomon and Carangelo, 1982; Solomonand and Carangelo, 1988; Ibarra et al., 1994; Ibarra and Moliner, 1994; Li et al., 2011; Yu et al., 2012), this paper describes the chemical functional groups of samples with the following parameters: the aromatic degree (f_a), the aliphatic hydrogen enrichment parameters (H_1 and H_2), the aliphatic chain structure parameter (T).

The calculation method is as follows:

A. aromatic degree (f_a) (Eqs. 1-3)

$$f_a = 1 - C_{al}/C \qquad (1)$$

$$C_{al}/C = [(H_{al}/H) \cdot (H/C)]/(H_{al}/C_{al}) \qquad (2)$$

C_{al}/C - ratio of aliphatic carbon to total carbon
H_{al}/H - ratio of aliphatic hydrogen to total hydrogen
H/C - ratio of total hydrogen to total carbon ;
H_{al}/C_{al} - ratio of aliphatic hydrogen to aliphatic carbon, generally taking 1.8 for coal
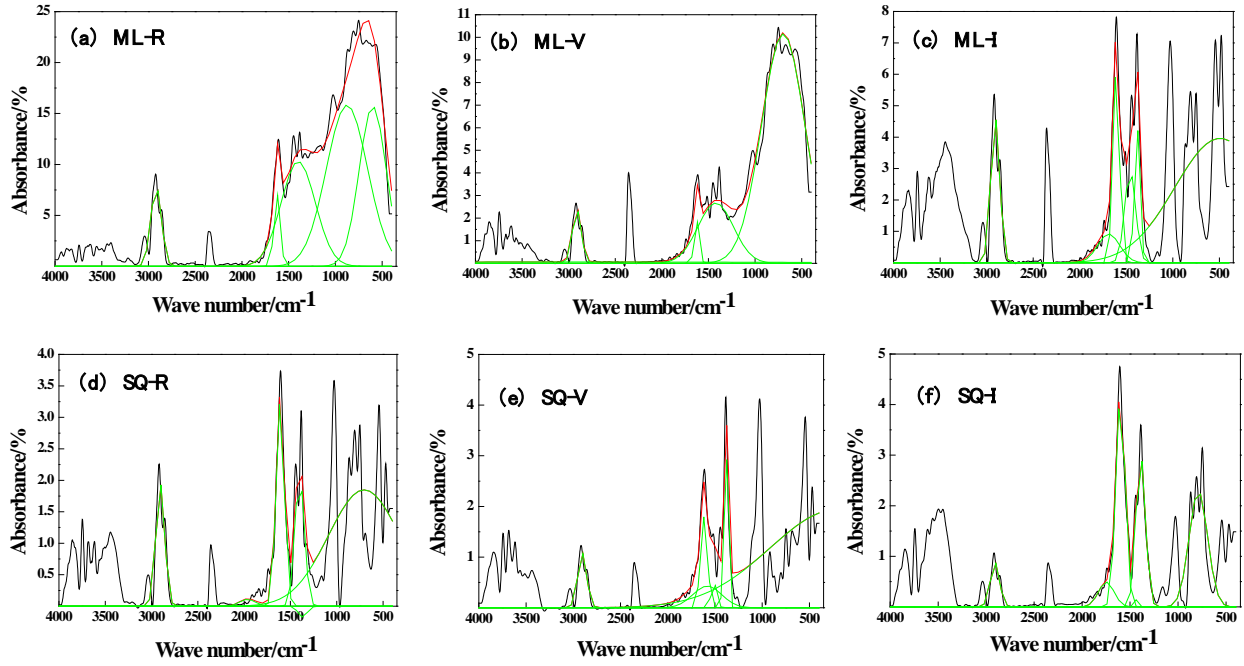
Fig. 4. Fitting charts of the peaks in the FTIR spectrum of coal samples with different macerals (a) Raw Malan coal, (b) Vitrinite-rich Malan coal, (c) Inertinite-rich Malan coal, (d) Raw Shaqu coal, (e) Vitrinite-rich Shaqu coal, (f) Inertinite-rich Shaqu coal

Table 4. The assignment and area of the peaks in the FTIR spectrum of coal samples with different maceral components (Painter et al., 1981, Painter et al., 1985; Wang and Griffith, 1985; Petersen et al., 2008)

Assignment ⟍ Sample number	Stretching vibration of aliphatic CH_2 and CH_3 ($A_{2800\text{-}3000}$)	Stretching vibration of aromatic $C = C$ (A_{1600})	Antisymmetric deformation vibration of aliphatic CH_2 and CH_3 ($A_{1430\text{-}1460}$)	Symmetrical bending vibration of aliphatic CH_3 (A_{1380})
	2800~3000 cm^{-1}	1595~1605 cm^{-1}	1430~1460 cm^{-1}	1370~1385 cm^{-1}
ML-R	977.355	89.021	386.333	227.557
ML-V	969.650	33.118	105.283	60.813
ML-I	970.414	88.625	155.792	102.253
SQ-R	219.902	34.728	65.472	42.759
SQ-V	209.880	24.006	46.297	29.908
SQ-I	96.027	44.323	63.095	49.203

$$H_{al} = A_{al}/a_{al} \qquad (3)$$

H_{al} - content of aliphatic hydrogen
A_{al} - the peak area of aliphatic hydrogen, taking the value of $A_{2800-3000}$;
a_{al} - the extinction coefficient, taking the value of 744 cm^{-1}

  B. aliphatic hydrogen enrichment parameters (H_1 and H_2) (Eq. 4)

$$\begin{cases} H_1 = A_{2800-3000}/A_{1600} \\ H_2 = (A_{2800-3000} + A_{1430-1460} + A_{1380})/A_{1600} \end{cases}$$
$$(4)$$

$A_{2800-3000}$ - peak area of stretching vibration of aliphatic CH_2 and CH_3;

A_{1600} - peak area of stretching vibration of aromatic C=C;

$A_{1430-1460}$ - peak area of antisymmetric deformation vibration of aliphatic CH_2 and CH_3;

A_{1380} - peak area of symmetrical bending vibration of aliphatic CH_3;

C. aliphatic chain structure parameter (T) (Eq. 5)

$$T = A_{1380}/A_{1430-1460} \qquad (5)$$

f_a represents the degree of aromatization; H_1 and H_2 represents the content of aliphatic hydrocarbon. T represents the length of aliphatic chain.
- the greater the value of H_1 or H_2 the higher the aliphatic hydrocarbon content.
- the higher value of the T reflects that more CH_3 is contained and the lower degree of branching, because the CH_3 has shorter length of chain branch than CH_2. The calculation results of relevant parameters are shown in Table 5.

Table 5. Infrared structural parameters of samples with different proportions of macerals

Sample number	Aromatic degree	Aliphatic hydrogen enrichment parameters		Aliphatic chain structure parameter
	f_a	H_1	H_2	T
ML-R	0.9035	10.9789	17.8749	0.5890
ML-V	0.9022	29.2786	34.2939	0.5776
ML-I	0.9036	10.9497	13.8613	0.6563
SQ-R	0.9785	6.3321	9.4487	0.6531
SQ-V	0.9784	8.7428	11.9172	0.6460
SQ-I	0.9905	2.1665	4.7002	0.7798

4. Discussion

The vitrinite-riched coal samples have shown the highest biomethane production, when inertinite-riched coal samples make the lowest(Fig.3). The major differences among the six types of samples (ML-R, ML-V, ML-I, SQ-R, SQ-V, SQ-I) are that they have different content of macerals. The content ratio of vitrinite to inertinite (V/I) in ML-R, ML-V, ML-I, SQ-R, SQ-V, SQ-I separately are 4.11, 6.83, 2.03, 3.98, 9.27 and 2.54. Comparing the ML-R, ML-V, ML-I, it can be seen that the biomethane production would increase when the V/I increases. The same trend exists in the SQ-R, SQ-V, SQ-I.

We believe that the differences of content and property of vitrinite and inertinite groups may have a significant effect on the biomethane generating capacity of the six samples. In addition, the liptinite possess a particularly low content in the coal compared to the other two macerals and did not exhibit the potential of biomethane in our experiment, So it would not consider as the key factor to biomethane generation. According to the aromatic degree(f_a), aliphatic hydrogen enrichment parameters (H_1 and H_2) and aliphatic chain structure parameter (T) (Fig. 5), the differences of chemical structure of the six samples were analyzed. By contrasting the samples from Malan coal(ML-R, ML-V, ML-I), the inertinite-rich coal sample(ML-I) has the highest f_a and vitrinite-rich Malan coal sample (ML-V) has the lowest f_a ; the inertinite-rich coal sample(ML-I) has the lowest H_1 and H_2 and the vitrinite-rich Malan coal sample (ML-V) has the highest H_1 and H_2; the inertinite-rich coal

sample (ML-I) has the highest T and the vitrinite-rich Malan coal sample (ML-V) has the lowest T. It indicates that the ML-V has the lower aromatization degree, higher content of aliphatic hydrocarbon and longer chain than ML-I.

The property of f_a , H_1 , H_2 ,and T of ML-R is in the middle of ML-V and ML-I. Comparing the f_a , H_1 , H_2 ,and T of samples from Shaqu coal(SQ-R, SQ-V, SQ-I), it also can be concluded that SQ-V has the lower aromatization degree, higher content of aliphatic hydrocarbon and longer chain than SQ-I. The higher ratio of CH_{al} /(CH_{al}+C=C) usually reflects the higher hydrocarbon generating potential in coals (Chen et al., 2012). Inertinite usually has a higher degree of aromatization, condensation and loss of heteroatoms (e.g., oxygen, sulfur, and nitrogen) than vitrinite, which may have resulted in a decrease in bioavailability (Robbins et al., 2016; Scott and Glasspool, 2007; Taylor et al., 1998). As a result, it has been assumed that coals of higher rank are less bioavailable due to the increase of aromaticity and condensation and will produce less methane than coals of lower rank (Fallgren et al., 2013; Strąpoć et al., 2011).

So we think that the difference of f_a , H_1 , H_2 and T which reflect the aromatization, content of aliphatic hydrocarbon and the length of chain branching influence the biodegradation of samples by methanogens and caused to the different biomethane production.

5. Conclusions

The biomethane generation and FTIR characteristic of samples from Malan and Shaqu mine were test in the laboratory, results show that vitrinite-rich coal samples make the higher biomethane yield than inertinite-rich coal samples and raw coal samples, when the samples were handled from the same coal mine.

Meanwhile, the vitrinite-rich coal samples have a higher content of aliphatic hydrocarbon and lower aromaticity than inertinite-rich coal samples by comparing the factors of f_a , H_1, H_2 and T. This indicates that the difference of macerals in coals would make a significant influence to the increase of biomethane resources in the coal bed.
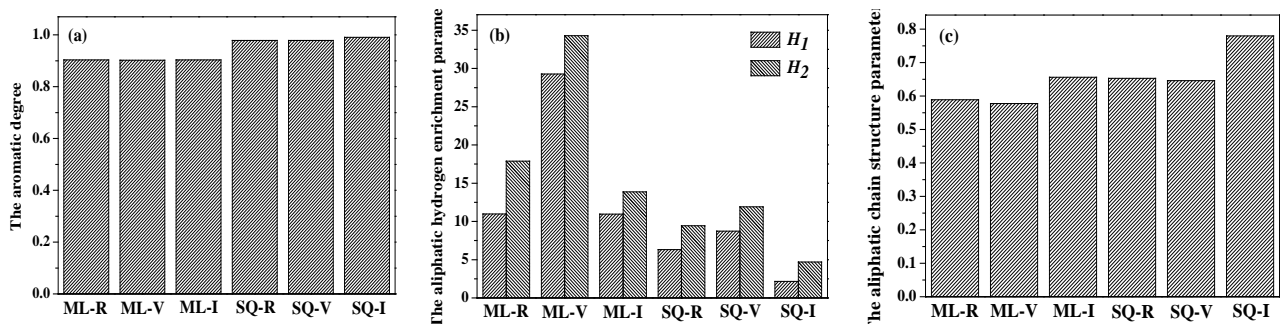

Fig. 5. (a) The aromatic degree (f_a) of different samples, (b) The aliphatic hydrogen enrichment parameters (H_1 and H_2) of different samples, (c) The aliphatic chain structure parameter (T) of different samples

Acknowledgements

References

Brenner D., (1984), *The Microscopic Infrared Spectroscopy of Coals*, In: *Chemistry and Characterization of Coal Macerals*, Winans, R.E., Crelling, J.C. (Eds.), ACS Symposium Series, American Chemical Society, Washington DC, **252**, 47-64.

Brown J.K., Lander W.R., (1960), A study of the hydrogen distribution in coal-like materials by high-resolution nuclear magnetic resonance spectroscopy. I. The measurement and interpreatation of the spectra, *Fuel*, **39**, 87-96.

Calabrò P.S., Panzera M.F., (2017), Biomethane production tests on ensiled orange peel waste, *International Journal of Heat and Technology*, **35**, 130-136.

Carotenuto C., Guarino G., Morrone B., Minale M., (2016), Temperature and pH effect on methane production from buffalo manure anaerobic digestion, *International Journal of Heat and Technology*, **34**, 425-429.

Chen H.B., Zhang Y.H., (2012), Research on separation and enrichment of macerals of coal, *Coal Quality Technology*, **11**, 6-9.

Chen Y., Mastalerz M., Schimmelmann A., (2012), Characterization of chemical functional groups in macerals across different coal ranks via micro-FTIR spectroscopy, *International Journal of Coal Geology*, **104**, 22-33.

Colosimo F., Thomas R., Lloyd J.R., Taylor K.G., Boothman C., Smith A.D., Lord R., Kalin R.M., (2016), Biogenic methane in shale gas and coal bed methane: A review of current knowledge and gaps, *International Journal of Coal Geology*, **165**, 106-120.

Fallgren P.H., Jin S., Zeng C.P., Ren Z.Y., Lu A.H., Colberg P.J.S., (2013), Comparison of coal rank for enhanced biogenic natural gas production, *International Journal of Coal Geology*, **115**, 92-96.

Fersiz S., Veli S., Turker M., Dagasan L., (2017), Anaerobic digestion of food waste from restaurant of a fermentation industry and potential for methane gas production, *Environmental Engineering and Management Journal*, **16**, 2001-2008.

Flores R.M., (2014), *Origin of Coal as Gas Source and Reservoir Rocks*, In: *Coal and Coalbed Gas*, Flores R.M. (Ed.), Elsevier, Amsterdam, 97-165.

Gilcrease P.C., Shurr G.W., (2007), Making microbial methane work: The potential for new biogenic gas, *World Oil*, **228**, 37-48.

Green M.S., Flanegan K.C., Gilcrease P.C., (2008), Characterization of a methanogenic consortium enriched from a coalbed methane well in the Powder River Basin, U.S.A, *International Journal of Coal Geology*, **76**, 34-45.

Guan D.S., (1990), Existing conditions for methanobacteria and biogenetic gases, *Nature Gas Industry*, **10**, 13-19.

Guo G.Y., Cao W.X., Sun S.Q., Zhao Y.J., Hu C.W., (2017), Nutrient removal and biogas upgrading by integrating fungal–microalgal cultivation with anaerobically digested swine wastewater treatment, *Journal of Applied Phycology*, **29**, 1-10.

Guo H.Y., Luo Y., Ma J.Q., Xia D.P., Ji C.J., Su X.B., (2014), Analysis of mechanism and permeability enhancing effect via microbial treatment on different-rank coals, *Journal of China Coal Society*, **39**, 1886-1891.

Guo Y., Bustin R.M., (1998), Micro-FTIR spectroscopy of liptinite macerals in coal, *International Journal of Coal Geology*, **36**, 259-275.

Guo Y., Renton, J.J., Penn, J.H., (1996), FTIR microspectroscopy of particular liptinite-lopinite rich, Late Permian coals from southern China, *International Journal of Coal Geology*, **29**, 187–197.

Hampartsoumian E., Nimmo W., Rosenberg P., Thomsen A., Williams, A., (1998), Evaluation of the chemical properties of coals and their maceral group constituents in relation to combustion reactivity using multi-variate analyses, *Fuel*, **77**, 735-748.

Ibarra J.V., Moliner R., Bonet A.J., (1994), FT-IR investigation on char formation during the early stages of coal pyrolysis, *Fuel*, **73**, 918-924.

Ibarra J.V., Munoz E., Moliner R., (1996), FTIR study of the evolution of coal structure during the coalification process, *Organic Geochemistry*, **24**, 725-735.

Kister J., Guiliano J.M., Largeau C., Derenne S., Casadevall E., (1990), Characterization of chemical structure, degree of maturation and oil potential torbanites-type 1 kerogen by quantitative FTIR spectroscopy, *Fuel*, **69**, 1357-1361.

Li Q.Z., Lin B.Q., Zhao C.S., Wu W.F., (2011), Chemical structure analysis of coal char surface based on fourier-transform infrared spectrometer, *Proceedings of the CSEE*, **31**, 46-52.

Li W.H., Chen Y.F., Chen W.M., Li X.L., (2000), Distribution features of micro-constituents for coal in China main mining area, *Coal Science and Technology*, **28**, 31-34.

Lin R., Ritz P., (1993a), Studying individual macerals using IR microspectroscopy, and implication on oil versus gasrcondense proneness and 'low-rank' generation. *Organic Geochemistry*, **20**, 695-706.

Lin R., Ritz P., (1993b), Reflectance FTIR microspectroscopy of fossil algae contained in organic-rich shales, *Applied Spectroscopy*, **47**, 265-271.

Mastalerz M., Bustin R.M., (1993a), Electron-microprobe and micro-FTIR analyses applied to maceral chemistry, *International Journal of Coal Geology*, **24**, 333-345.

Mastalerz M., Bustin R.M., (1993b), Variation in maceral chemistry within and between coals of varying rank: an electronic microprobe and micro-Fourier transform infrared investigation. *Journal of Microscopie*, **171**, 153-166.

Mastalerz M., Bustin R.M., (1996), Application of reflectance micro-Fourier Transform infrared analysis to the study of coal macerals: an example from the Late Jurassic to Early Cretaceous coals of the Mist Mountain Formation, British Columbia, Canada, *International Journal of Coal Geology*, **32**, 55-67.

Mazzeo R., Joseph E., (2007), Attenuated total reflectance microspectroscopy mapping for the characterization of bronze corrosion products, *European Journal of Mineralogy*, **19**, 363-371.

Messenböck R.C., Paterson N.P., Dugwell D.R., Kandiyoti R., (2000), Factors governing reactivity in low temperature coal gasification. Part 1. An attempt to

correlate results from a suite of coals with experiments on maceral concentrates, *Fuel*, **79**, 109-121.

Millais R., Murchison D.G., (1969), Properties of the coal macerals: Infrared spectra of alginites, *Fuel*, **48**, 247-258.

Moore, T.A., (2012), Coalbed methane: A review, *International Journal of Coal Geology*, **101**, 36-81.

Morga R., (2010), Chemical structure of semifusinite and fusinite of steam and coking coal from the Upper Silesian Coal Basin (Poland) and its changes during heating as inferred from micro-FTIR analysis. *International Journal of Coal Geology*, **84**, 1-15.

Painter P., Starsinic M., Coleman M., (1985), *Determination of Functional Groups in Coal by Fourier Transform Interferometry*, In: *Fourier Transform Infrared Spectra Applications to Chemical Systems*, Volume 4, Ferraro J.R., Basile L.J. (Eds.), Academic Press, 169-241.

Painter P.C., Snyder R.W., Starsinic M., Coleman M.M., Kuehn D.W., Davis A., (1981), Concerning the application of FT-IR to the study of coal: a critical assessment of band assignments and the application of spectral analysis programs, *Applied Spectroscopy*, **35**, 475-485.

Papendick S.L., Downs K.R., Vo K.D., Hamilton S.K., Dawson K.W., Golding S.D., Gilcrease P.C., (2011), Biogenic methane potential for Surat Basin, Queensland coal seams, *International Journal of Coal Geology*, **88**, 123-134.

Penner T.J., Foght J.M., Budwill K., (2010), Microbial diversity of western Canadian subsurface coal beds and methanogenic coal enrichment cultures, *International Journal of Coal Geology*, **82**, 81-93.

Petersen, H.I., Rosenberg, P., Nytoft, H.P., (2008), Oxygen groups in coals and alginite-rich kerogen revisited, *International Journal of Coal Geology*, **74**, 93-113.

Robbins, S.J., Evans, P.N., Esterle, J.S., Golding, S.D., Tyson, G.W., (2016), The effect of coal rank on biogenic methane potential and microbial composition, *International Journal of Coal Geology*, **154-155**, 205-212.

Rochdi, A., Landais, P., (1991), Transmission micro-infrared spectroscopy, an efficient tool for microscale characterization of coal, *Fuel*, **70**, 364-371.

Scott, A.C., Glasspool, I.J., (2007), Observations and experiments on the origin and formation of inertinite group macerals, *International Journal of Coal Geology*, **70**, 53-66.

Solomon P.R., Carangelo R.M., (1982), FTIR analysis of coal. 1. Techniques and determination of hydroxyl concentrations, *Fuel*, **61**, 663-669.

Solomon P.R., Carangelo R.M., (1988), FT-IR analysis of coal: 2. Aliphatic and aromatic hydrogen concentration, *Fuel*, **67**, 949-959.

Strąpoć D., Mastalerz M., Katherine D., Macalady J., Callaghan A.V., Wawrik B., Turich C., Ashby M., (2011), Biogeochemistry of Microbial Coal-Bed Methane, *Annual Review of Earth & Planetary Sciences*, **39**, 617-656.

Su X.B., Xu Y., Wu Y., Xia D.P., Chen X., (2011), Effect of salinity and pH on biogenic methane production of low-rank coal, *Journal of China Coal Society,* **36**, 1302-1306.

Sun Q.L., Li W., Chen H.K., Li B.Q., (2003), The variation of structure characterization of macerals during pyrolysis, *Fuel*, **82**, 669-676.

Sun X.G., (2005), The investigation of chemical structure of coal macerals via transmitted-light FT-IR microspectroscopy, *Spectrochimica Acta Part A: Molecular and Biomolecular Spectroscopy*, **62**, 557-564.

Susilawati R., Papendick S.L., Gilcrease P.C., Esterle J.S., Golding S.D., Mares T.E., (2013), Preliminary investigation of biogenic gas production in Indonesian low rank coals and implications for a renewable energy source, *Journal of Asian Earth Sciences*, **77**, 234-242.

Taylor G.H. (Ed.), (1998), *Organic Petrology: a New Handbook Incorporating Some Revised Parts of Stach's Textbook of Coal Petrology*, Gebrüder Borntraeger, Stuttgart, Germany.

Tschamiler H., Ruiter E.D., (1966). A comparative study of exinite, vitrinite and micrinite, *Advances in Chemical Physics*, **55**, 332-343.

Ulrich G., Bower S., (2008), Active methanogenesis and acetate utilization in Powder River Basin coals, United States, *International Journal of Coal Geology*, **76**, 25-33.

Van Krevele D.W., (1961), *Coal*, Elsevier, Amsterdam.

Vasmara C., Marchetti R., (2016), biogas production from biodegradable bioplastics, *Environmental Engineering and Management Journal*, **16**, 2041-2048.

Walker R., Mastalerz M., (2004), Functional group and individual maceral chemistry of high volatile bituminous coals from southern Indiana: controls on coking. *International Journal of Coal Geology*, **58**, 181-191.

Wang A.K., Qin Y., Shao P., (2015), Effect characteristics of coal particle size on lignite generation, *China Coalbed Methane*, **12**, 3-6.

Wang G.J., (1992), Study on chemical structure of Xiqu coal macerals, *Journal of China University of Mining & Technology*, **21**, 97-103.

Wang S.H., Griffiths P.R., (1985), Resolution enhancement of diffuse reflectance IR spectra of coals by Fourier self-deconvolution. 1. C-H stretching and bending modes, *Fuel*, **64**, 229-236.

Xia D.P., Chen X., Su, X.B., Wu Y., (2012), Impact of oxidation-reduction potential on the generation of biogenic methane in low-rank coals, *Natural Gas Industry*, **32**, 107-110.

Xie K.C., (2002), *Coal Structure and its Reactivity*, Science Press, Beijing, China.

Yu X.L., Bai F., Li Z.M., (2012), Application of attenuated total reflectance-micro-Fourier transform infrared (ATR-FTIR) spectroscopy to in-situ study of coal macerals, *Petroleum Geology & Experiment*, **34**, 664-670.

Zhao F.H., Ren D.Y., (1995). The application of high-resolution transmission electron microscopy to study the structures of coal macerals, *Geological Review*, **41**, 564-571.

Zhou Y.J., (2013), Study on separation macerals in Shenfu coal by flotation, Xi'an University of Science and Technology, China.